

GAS HOLDUP AND VOLUMETRIC LIQUID-PHASE MASS TRANSFER COEFFICIENT IN SOLID-SUSPENDED BUBBLE COLUMN WITH DRAUGHT TUBE

KOZO KOIDE, KAZUYOSHI HORIBE, HIROKAZU KAWABATA
AND SHIGETAKA ITO

Department of Chemical Engineering, Shizuoka University, Hamamatsu 432

Key Words: Mass Transfer, Bubble Column, Draught Tube, Solid Particles, Gas Holdup, Slurry Reactor

The effects of column dimensions, gas velocity and properties of the liquid and the solid particles on the gas holdup ε_G and the volumetric liquid-phase mass transfer coefficient $k_L a$ in a solid suspended bubble column with a draught tube and a conical bottom were studied experimentally in a liquid-solid batch operation. The presence of suspended solid particles in the column reduces the values of ε_G and $k_L a$, and their reduction due to the addition of solid particles to the column increases with increasing solid concentration and terminal velocity of a single particle. Based on these observations, empirical equations for ε_G and $k_L a$ are proposed which are applicable to columns with diameter of 0.1–0.3 m.

Introduction

The solid-suspended bubble column with a draught tube and a conical bottom (usually with a $\pi/3$ rad angle) is often called the pachuca tank and is used widely as an apparatus for leaching ores.⁸⁾ To design a column of this type as a slurry reactor, the average gas holdup ε_G and the volumetric liquid-phase mass transfer coefficient $k_L a$ should be known. Muroyama *et al.*¹⁰⁾ have shown that ε_G and $k_L a$ in a column of this type agree with those in a bubble column without draught tube, and the effect of the solid concentration on ε_G and $k_L a$ is ignored. Further, they have proposed an empirical equation for $k_L a$. However, this equation is applicable only to a slurry of water-activated carbon particles, and the effects of properties of the liquid and the solid particles on $k_L a$ are not clear.

The purpose of this study is to clarify experimentally the effects of column dimensions, gas velocity and properties of the liquid and the solid particles on ε_G and $k_L a$ in the solid-suspended bubble column with a draught tube and with a conical bottom in liquid-solid batch operation.

1. Experimental

The experimental apparatus used in this work is shown in Fig. 1. The dimensions of the plexiglass column used are shown in Table 1. As shown in Fig. 1(b), the column bottom consists of a conical section with a cone angle of $\pi/3$ rad, and a perforated plate is used as gas distributor. The perforated plate is cov-

ered with a stainless steel wire gauze of 260–300 mesh to prevent solid particles from penetrating to the gas distributor through the holes, and the holes of the gas distributor are oriented in triangular pitches. Details of the gas distributors are shown in Table 2.

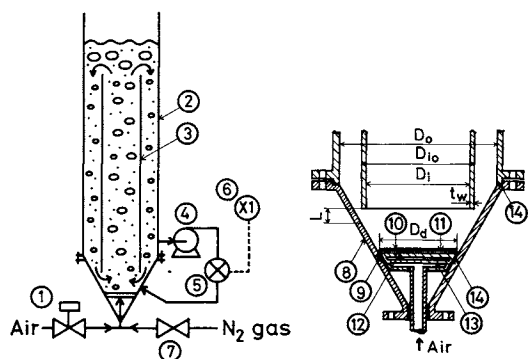
The liquids used in this work were demineralized water and aqueous solutions of glycerol, glycol, barium chloride and sodium sulfate. The values for the static slurry height H_L above the gas distributor are shown in Table 1. The operating temperature was kept at 298.2 ± 0.5 K. Tables 3 and 4, respectively, show physical properties of the liquids and of glass and bronze spheres used in this work. The average diameter d_p of solid particles and the terminal velocity V_t of a single particle were obtained by the same methods as those discussed in the previous paper.³⁾ The average solid concentration c_s in gas-free slurry was varied in the range of 0–200 kg·m⁻³, and air was dispersed into the column through a gas distributor at a gas velocity sufficient to suspend all the solid particles in the column. During each run liquid and solid particles were neither fed nor discharged.

The average gas holdup ε_G was calculated by Eq. (1), using data of H_L and aerated slurry height H_F determined by visual observation.

$$\varepsilon_G = \frac{(H_F - H_L)}{\left\{ H_F - \frac{\sqrt{3}}{2} (D_o - D_d) \right\} + \frac{\sqrt{3}}{6D_o^2} \{ D_o^3 - D_d^3 \} - \frac{V_t}{S_o}} \quad (1)$$

The physical absorption of oxygen in the air by the liquid was employed to determine $k_L a$. The details of this method are similar to those discussed in the previous papers.^{6,7)}

Received September 28, 1984. Correspondence concerning this article should be addressed to K. Koide, Dept. of Chem. Eng., Tokyo Inst. of Tech., 2-12-1 Ookayama, Meguro-ku, Tokyo 152. K. Horibe is now with Nippon Steel Corp. Himeji 671-11. S. Ito is now with Engineering Plastics, Ltd., Gotemba 412.



(a) Experimental apparatus (b) Details of gas distributor

Fig. 1. Experimental apparatus and details of gas distributor. 1, solenoid valve; 2, column; 3, draught tube; 4, pump; 5, oxygen sensor; 6, oxygen meter; 7, valve; 8, conical bottom; 9, gas distributor; 10, stainless steel rim; 11, stainless steel gauze; 12, perforated plate; 13, buffer plate; 14, rubber packing.

Table 1. Experimental apparatus

D_o [m]	D_i^* [m]	H [m]	H_L [m]	$L \times 10^2$ [m]	Perforated plate**
0.100	0.060	1.40	1.50	2.1	P1
0.140	0.066	1.40	1.54	3.0	P1
0.140	0.082	0.70–2.10	0.84–2.24	0.34–4.4	P1, P2, P3
0.140	0.094	1.40	1.54	3.0	P1
0.140	0.104	1.40	1.54	3.0	P1
0.218	0.128	1.40	1.58	4.8	P4
0.300	0.190	1.40	1.68	6.2	P4

* $t_w = 3$ mm for $D_i \leq 0.128$ m and 5 mm for $D_i = 0.190$ m.

** Dimensions of perforated plates are shown in Table 2.

Table 2. Dimensions of perforated plates

Gas distributor	D_d [m]	δ [mm]	N [—]
P1	0.035	3	3
P2	0.050	3	7
P3	0.070	3	7
P4	0.086	3	10

2. Results and Discussion

2.1 Experimental results of ε_G and $k_L a$

Experimental results of ε_G and $k_L a$ shown in this paper were obtained under conditions such that all the solid particles were suspended in the column.

Figure 2 shows that both ε_G and $k_L a$ increase with increasing U_G and decrease with increasing solid concentration c_s .

Figure 3 shows that both ε_G and $k_L a$ decrease with increasing terminal velocity V_t of a single particle. However, $k_L a$ in slurries of bronze spheres ($\rho_s = 8770$ kg·m⁻³) are slightly higher than those in slurries of glass spheres ($\rho_s = 2500$ kg·m⁻³) at the same values of

Table 3. Properties of liquids at 298.2 K

Liquid*	ρ_L [kg·m ⁻³]	$\mu_L \times 10^3$ [Pa·s]	$\sigma_L \times 10^3$ [N·m ⁻¹]	$D_L \times 10^9$ [m ² ·s ⁻¹]	Crk^2/σ_L [—]
W	997	0.894	72.0	2.42	0
100BC	1016	0.919	72.4	2.35	6.25
270BC	1048	0.957	73.0	2.25	16.9
400SS	1047	1.05	73.0	2.06	25.4
39GL	1098	2.88	68.8	0.749	33.5
55GL	1140	5.18	68.2	0.404	95.9
71GL	1182	17.0	65.0	0.145	38.7
73EG	1088	5.25	51.5	0.439	58.7

* W: water; 100BC and 270BC: 100 and 270 mol·m⁻³ BaCl₂ aq. solns; 400SS: 400 mol·m⁻³ Na₂SO₄ aq. soln; 39GL, 55GL and 71GL: 39.4, 54.7 and 70.5 wt% glycerol aq. solns; 73EG: 72.9 wt% ethylene glycol aq. soln.

Table 4. Properties of solid particles

Material	Size [mesh]	d_p [μm]	$V_t \times 10^2$ [m·s ⁻¹]
Glass sphere $\rho_s = 2500$ kg·m ⁻³	60–80	198	2.44 (in water)
	60–80	198	2.37 (in 100BC)
	60–80	198	2.26 (in 270BC)
	60–80	198	2.13 (in 400SS)
	60–80	198	0.990 (in 39GL)
	60–80	198	0.472 (in 55GL)
	60–80	198	0.165 (in 71GL)
	60–80	198	0.548 (in 73EG)
	80–100	136	1.40 (in water)
High index Glass sphere $\rho_s = 4680$ kg·m ⁻³	100–140	117	1.09 (in water)
	140–200	79.0	0.555 (in water)
Bronze sphere $\rho_s = 8770$ kg·m ⁻³	140–200	89.0	2.91 (in water)

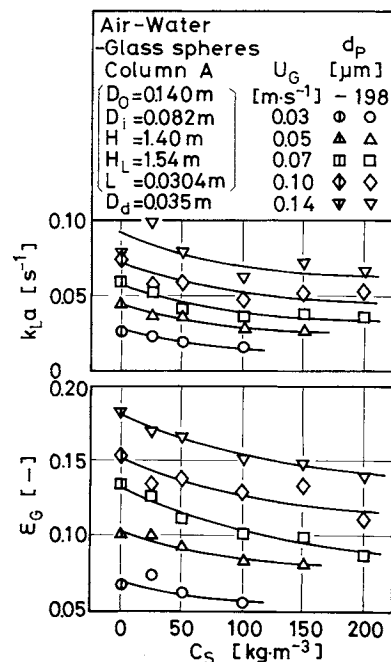


Fig. 2. Effects of gas velocity and solid concentration on ε_G and $k_L a$.

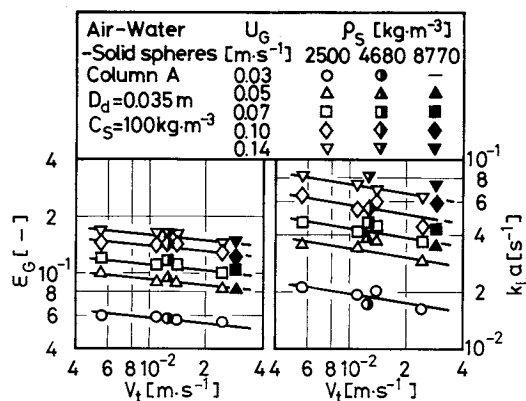


Fig. 3. Effect of terminal velocity of a single particle on ϵ_G and k_La .

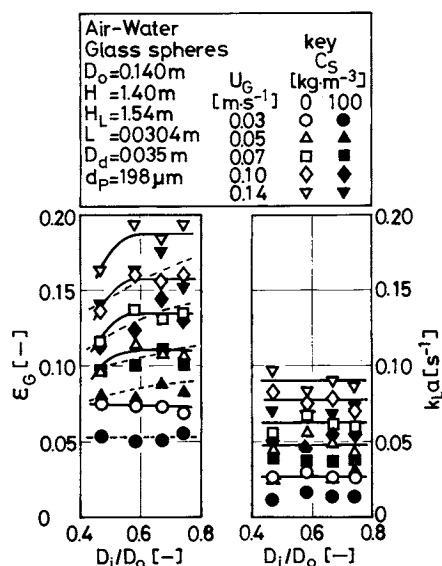


Fig. 4. Effect of draught tube diameter on ϵ_G and k_La .

V_t , U_G and c_s . This suggests that the effect of solid particles on k_La might be expressed better by the volume fraction (c_s/ρ_s) rather than by c_s .

Figure 4 shows that ϵ_G is slightly higher in the column having larger value of D_i/D_o in the range of $U_G > 0.05 \text{ m.s}^{-1}$. This might be due to the fact that for the same D_o the column having a large value of D_i/D_o has a large cross-sectional area in the draught tube, where the gas holdup is larger than that in the annulus. On the other hand, D_i/D_o has almost no effect on k_La . This might be due to the fact that the column having larger value of D_i/D_o has smaller cross-sectional area of the annulus where the specific gas-liquid interfacial area is larger than that in the draught tube.⁴⁾

Figure 5 shows that the length of the draught tube H and H_L have almost no effect on ϵ_G and k_La .

Figure 6 shows that when D_i/D_o is constant, the inner diameter D_o of the column has no effect on ϵ_G , but that k_La increases with increasing D_o . The circulating liquid flow in the larger column seems more

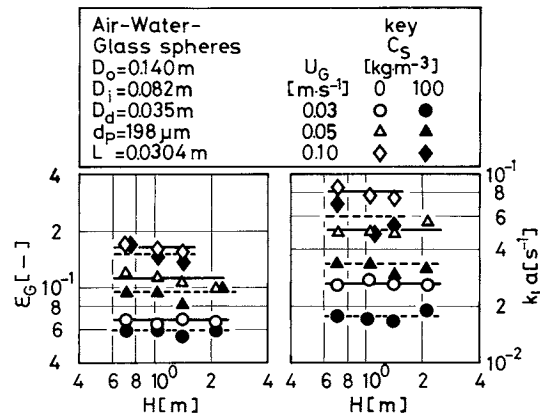


Fig. 5. Effect of clear liquid height on ϵ_G and k_La .

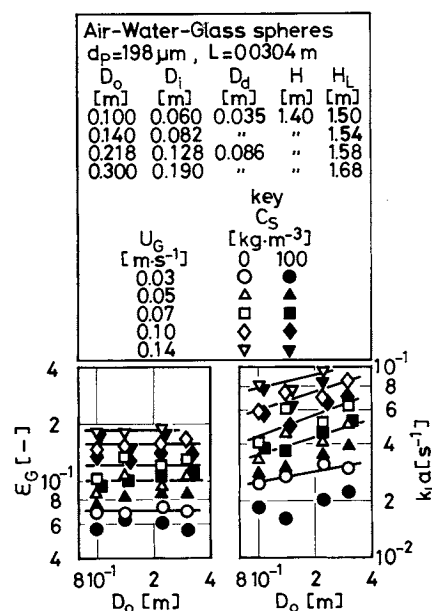


Fig. 6. Effect of column diameter on ϵ_G and k_La .

turbulent near the lower end of the draught tube, and this might enhance the gas-liquid mass transfer in a larger column.

Vertical clearance L between the lower end of the draught tube and the wall of the conical bottom had no effect on ϵ_G and k_La in the range of $L/D_i = 0.04$ – 0.54 . Also, the diameter D_d of the perforated plate had no effect on ϵ_G and k_La in the range $D_d/D_o = 0.25$ – 0.50 .

Figure 7 shows that the values of ϵ_G and k_La in BaCl_2 and Na_2SO_4 aqueous solutions are higher than those in water. This might be due to the fact that in these solutions bubble coalescence is hindered and then bubble sizes are smaller than those in water. This figure shows also that the values of ϵ_G and k_La in 55 wt.% glycerol aqueous solution are higher than those in 39 wt.% glycerol aqueous solution, though the viscosity of the former solution is higher than that of the latter. This indicates that the frothing ability of the liquid affects the values of ϵ_G and k_La in these

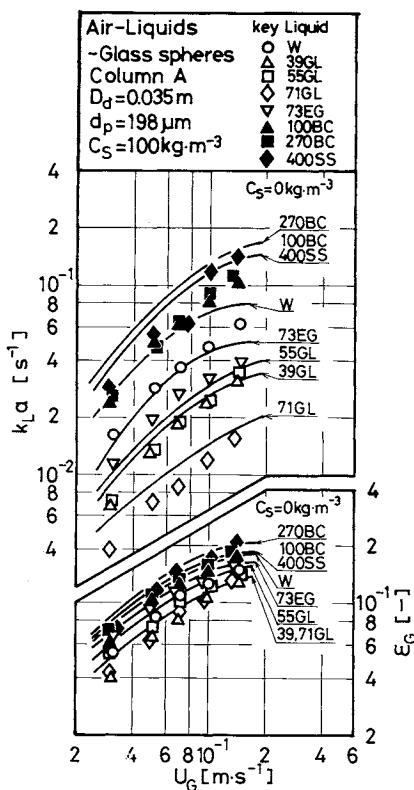


Fig. 7. Effect of liquid properties on ε_G and k_La .

solutions, as was pointed out in the previous papers.^{5,6} Further, comparisons of ε_G and k_La in glycol aqueous solution with those in 55 wt.% glycerol aqueous solution show that both ε_G and k_La increase with decreasing liquid surface tension.

2.2 Correlations of ε_G and k_La

Firstly, ε_G and k_La in columns without solid particles were correlated with experimental conditions. Secondly, these correlations of ε_G and k_La were modified to include the effect of solid particles on ε_G and k_La .

The observations above show that ε_G for $c_s=0$ increases with increasing U_G , D_i/D_o and frothing ability of the liquid and with decreasing μ_L and σ_L . Since the effects of these parameters on ε_G were similar to those in the column with a draught tube and a flat bottom,⁵ an empirical formula correlating ε_G similar to that reported in the previous paper⁵ was assumed. Numerical constants in the following empirical equation of ε_G were decided by the direct search method²) using the data observed in this work, where the frothing ability of the liquid was expressed by Marrucci's parameter,⁹ Crk^2/σ_L .*

$$\left[\frac{\varepsilon_G}{(1-\varepsilon_G)^4} \right]_0 = \frac{0.127 \left(\frac{U_G \mu_L}{\sigma_L} \right)^{0.934} \left(\frac{\rho_L \sigma_L^3}{g \mu_L^4} \right)^{0.292} \left(\frac{D_i}{D_o} \right)^{0.300}}{\left[1 - 0.196 \left\{ 1 - \exp \left(-0.135 \frac{Crk^2}{\sigma_L} \right) \right\} \right]^{-1}} \quad (2)$$

* Details of determining this parameter are shown in the previous paper.⁶

The effect of solid particles in reducing ε_G value increases with increasing c_s and V_t and with decreasing U_G and σ_L . Therefore, Eq. (2) was modified to Eq. (3), where the numerical constants of the terms in the last brace were decided by the direct search method²) using the data for $c_s \neq 0$.

$$\begin{aligned} \frac{\varepsilon_G}{(1-\varepsilon_G)^4} &= 0.127 \left(\frac{U_G \mu_L}{\sigma_L} \right)^{0.934} \left(\frac{\rho_L \sigma_L^3}{g \mu_L^4} \right)^{0.292} \left(\frac{D_i}{D_o} \right)^{0.300} \\ &\times \left[1 - 0.196 \left\{ 1 - \exp \left(-0.135 \frac{Crk^2}{\sigma_L} \right) \right\} \right]^{-1} \\ &\times \left\{ 1 + 0.17 \left(\frac{C_s}{\rho_s} \right)^{0.091} \left(\frac{\rho_L \sigma_L^3}{g \mu_L^4} \right)^{0.043} \left(\frac{V_t}{U_G} \right)^{0.067} \right\}^{-1} \quad (3) \end{aligned}$$

The average error in estimating ε_G by Eq. (3) was within 12% for 383 data in the experimental ranges of

$$\begin{aligned} 3.59 \times 10^{-4} &\leq (U_G \mu_L / \sigma_L) \leq 3.70 \times 10^{-2}, \\ 1.69 \times 10^{-11} &\leq (g \mu_L^4 / \rho_L \sigma_L^3) \leq 2.55 \times 10^{-6}, \\ 0.471 &\leq (D_i / D_o) \leq 0.743, \\ 0 &\leq (Crk^2 / \sigma_L) \leq 95.9, \\ 0 &\leq (c_s / \rho_s) \leq 8.00 \times 10^{-2} \end{aligned}$$

and

$$1.17 \times 10^{-2} \leq (V_t / U_G) \leq 0.844.$$

Figure 8 shows that ε_G values estimated by Eq. (3) agree relatively well with those observed experimentally.

k_La for $c_s=0$ increases with increasing U_G , D_o and frothing ability of the liquid and with decreasing μ_L and σ_L . As Akita *et al.*¹) have shown that a better empirical equation of k_La is obtained by using ε_G instead of U_G in a bubble column without a draught tube, $\log k_La$ is plotted against $\log \varepsilon_G$ in Fig. 9, which yields straight lines of the slope of 1.34. Therefore, the following empirical equation of k_La for $c_s=0$ was obtained by dimensional analysis and the least squares method, using ε_G instead of U_G , where the exponent of Schmidt number ($\mu_L / \rho_L D_L$) was assumed to be 0.5 as was done by Akita *et al.*¹)

$$\begin{aligned} \frac{(k_La)_0 D_o^2}{D_L} &= 2.66 \left(\frac{\mu_L}{\rho_L D_L} \right)^{0.500} \left(\frac{g D_o^2 \rho_L}{\sigma_L} \right)^{0.715} \\ &\times \left(\frac{g D_o^3 \rho_L^2}{\mu_L^2} \right)^{0.251} \left(\frac{D_i}{D_o} \right)^{-0.429} \varepsilon_G^{1.34} \quad (4) \end{aligned}$$

The effect of solid particles on reducing k_La value increases with increasing c_s and V_t . As shown in Fig. 9 the relations of $\log k_La$ vs. ε_G are linear also for $c_s \neq 0$, and the slope of these lines is about 1.34. However, the value of k_La for $c_s \neq 0$ is slightly lower than that for $c_s=0$ at the same value of ε_G . Therefore, the equation in the form of Eq. (5) was assumed to modify Eq. (4) by taking the effect of solid particles

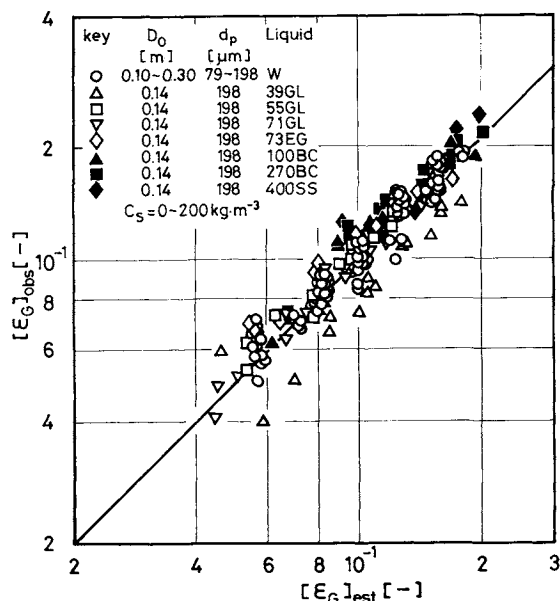


Fig. 8. Comparison of ε_G values estimated by Eq. (3) with those observed in this work.

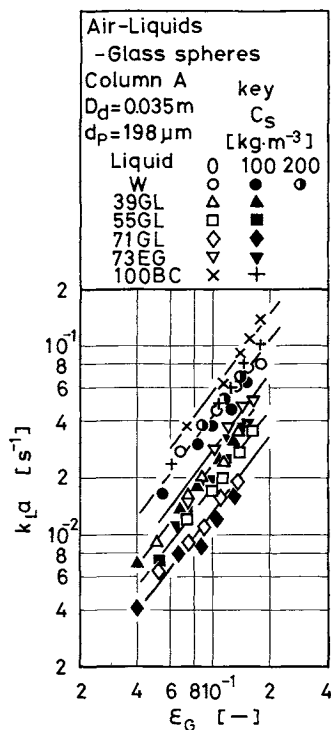


Fig. 9. k_La vs. ε_G .

on k_La into consideration. The numerical constants of the brace in Eq. (5) were decided by the direct search method²⁾ using data for $c_s \neq 0$.

$$\frac{k_LaD_o^2}{D_L} = 2.66 \left(\frac{\mu_L}{\rho_L D_L} \right)^{0.500} \left(\frac{gD_o^2 \rho_L}{\sigma_L} \right)^{0.715} \times \left(\frac{gD_o^3 \rho_L^2}{\mu_L^2} \right)^{0.251} \left(\frac{D_i}{D_o} \right)^{-0.429} \varepsilon_G^{1.34}$$

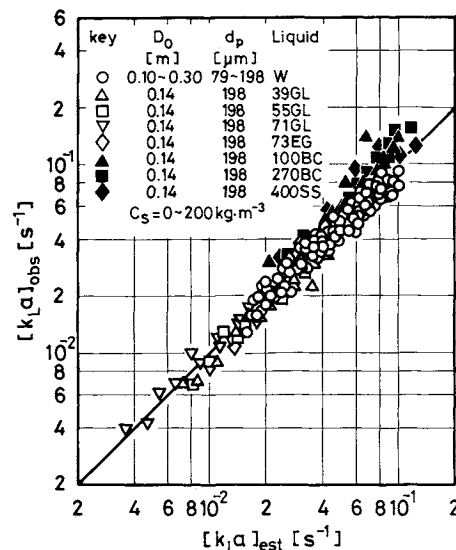


Fig. 10. Comparison of k_La values estimated by Eq. (5) with those observed in this work.

$$\times \left\{ 1 + 0.099 \left(\frac{c_s}{\rho_s} \right)^{0.069} \left(\frac{\rho_L \sigma_L^3}{g \mu_L^4} \right)^{0.023} \left(\frac{V_t}{U_G} \right)^{0.046} \right\}^{-1} \quad (5)$$

The average error in estimating k_La by Eq. (5) was within 17% for 383 data in the experimental ranges of

$$3.71 \times 10^2 \leq (\mu_L / \rho_L D_L) \leq 9.92 \times 10^4,$$

$$1.36 \times 10^3 \leq (g D_o^2 \rho_L / \sigma_L) \leq 1.22 \times 10^4,$$

$$1.29 \times 10^8 \leq (g D_o^3 \rho_L^2 / \mu_L^2) \leq 1.26 \times 10^{11},$$

$$0.471 \leq (D_i / D_o) \leq 0.743,$$

$$3.99 \times 10^{-2} \leq \varepsilon_G \leq 2.73 \times 10^{-1},$$

$$0 \leq (c_s / \rho_s) \leq 8.00 \times 10^{-2},$$

$$1.69 \times 10^{-11} \leq (g \mu_L^4 / \rho_L \sigma_L^3) \leq 2.55 \times 10^{-6}$$

and

$$1.17 \times 10^{-2} \leq (V_t / U_G) \leq 0.844.$$

Figure 10 shows that k_La values estimated by Eq. (5) agree relatively well with those observed experimentally.

2.3 Comparison of this work with the previous ones

For $c_s = 0$ and at the same gas velocity, k_La in the column (column A) used in this work is larger than that in the column (column B) with a draught tube, a flat bottom and gas dispersion into the tube.⁵⁾ This might be due to the fact that the dead water region which exists near the periphery of the flat bottom of column B doesn't exist in column A. Meanwhile, k_La in column A without solid particles is roughly equal to that in the column with a draught tube and gas dispersion into the annulus,⁶⁾ though ε_G is smaller in the former column than in the latter.

Muroyama *et al.*¹⁰⁾ have reported that k_La in a

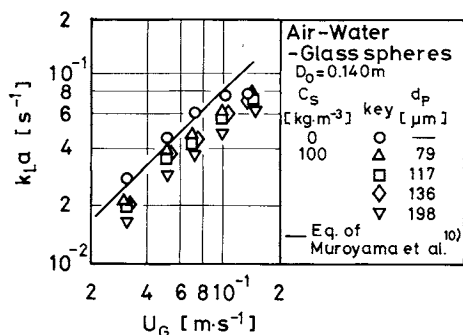


Fig. 11. Comparison of k_La values estimated by the equation of Muroyama *et al.*¹⁰⁾ with those observed in this work.

column similar to that used in this work is not affected by (c_s/ρ_s) and increases with increasing gas velocity and column diameter. Further, they have proposed an empirical equation for k_La in the air-water-activated carbon particles system. Figure 11 shows that the equation agrees relatively well with k_La in column A without solid particles. However, the equation doesn't agree with k_La values observed in column A with slurries of glass particles. This discrepancy might be due to the fact that the equation is based on data of k_La for slurries of activated carbon of which the density ($\rho_s \approx 1300 \text{ kg} \cdot \text{m}^{-3}$) is much lower than that of glass particles ($\rho_s \approx 2500 \text{ kg} \cdot \text{m}^{-3}$).

For $c_s = 0$, k_La values estimated by Eq. (5) for column A agree with those observed in the bubble column (column C) without a draught tube and with a perforated plate as gas distributor. However, Fig. 12 shows that for $c_s \neq 0$ the values of k_La in column A are much larger than those in column C, when a liquid of high viscosity is used. Considering this phenomenon and the fact that solid particles are suspended with lower gas velocity and more uniformly in column A than in column C,³⁾ the former column is more suitable as a slurry reactor than the latter.

Conclusions

The presence of suspended solid particles in the bubble column with a draught tube and a conical bottom reduces values of the gas holdup ε_G and the volumetric liquid-phase mass transfer coefficient k_La . The reduction of ε_G and k_La values due to an addition of solid particles to the column increases with increasing solid concentration and terminal velocity of a single particle. Based on these observations, empirical equations of ε_G and k_La are proposed.

The bubble column with a draught tube and a conical bottom is more suitable as a slurry reactor than one without a draught tube since the solid particles are suspended with a lower gas velocity and are distributed more uniformly within the column, and the values of k_La for slurries of high viscosity are larger in the former column than in the latter.

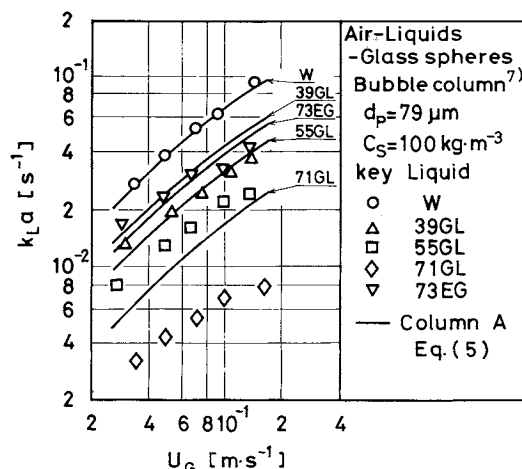


Fig. 12. Comparison of k_La values in bubble columns with and without draught tube. $D_0 = 0.14 \text{ m}$.

Nomenclature

A	= Hamaker constant	[J]
a	= specific gas-liquid interfacial area based on aerated liquid volume	[m ⁻¹]
C	= $\frac{2c_1}{vRT} \left(\frac{d\sigma_L}{dc_1} \right)^2 \frac{1}{\{1 + (d \ln f_1 / d \ln c_1)\} \{1 + (x_1 v_1 / x_2 v_2)\}}$	[N]
Crk^2/σ_L	= parameter of bubble coalescence proposed by Marrucci ^{6,9)}	[—]
c_s	= $\rho_s \varepsilon_s / (\varepsilon_L + \varepsilon_s)$, average solid concentration in gas-free slurry	[kg · m ⁻³]
c_1	= concentration of component 1 in liquid	[mol · m ⁻³]
D_d	= diameter of gas distributor	[m]
D_i	= inner diameter of draught tube	[m]
D_{io}	= $D_i + 2t_w$, outer diameter of draught tube	[m]
D_L	= diffusivity of dissolved oxygen	[m ² · s ⁻¹]
D_o	= column diameter	[m]
d_p	= average diameter of solid particles	[m]
f_1	= activity coefficient of component 1 in liquid	[—]
g	= gravitational acceleration	[m · s ⁻²]
H	= length of draught tube	[m]
H_F	= level of aerated slurry during operation	[m]
H_L	= static slurry height above gas distributor	[m]
k	= $(12\pi\sigma_L/Ar)^{1/3}$	[m ⁻¹]
k_L	= liquid-phase mass transfer coefficient	[m · s ⁻¹]
k_La	= volumetric liquid-phase mass transfer coefficient based on aerated slurry volume	[s ⁻¹]
L	= vertical clearance between lower end of draught tube and wall of conical bottom shown in Fig. 1(b)	[m]
N	= number of holes in gas distributor	[—]
P	= pitch of holes in gas distributor	[m]
R	= gas constant	[J · K ⁻¹ · mol ⁻¹]
r	= radius of bubble	[m]
S_o	= cross-sectional area of column	[m ²]
T	= liquid temperature	[K]
t_w	= wall thickness of draught tube	[m]
U_G	= gas velocity based on cross section of column and based on average static pressure in column	[m · s ⁻¹]
V_i	= volume of draught tube	[m ³]
V_t	= terminal velocity of a single particle in stagnant liquid	[m · s ⁻¹]

v_1, v_2	= molar volume of components 1 and 2 in liquid	$[\text{m}^3 \cdot \text{mol}^{-1}]$
x_1, x_2	= mole fraction of components 1 and in liquid	[—]
δ	= hole diameter in gas distributor	[m]
ε_G	= gas holdup	[—]
ε_L	= liquid holdup	[—]
ε_S	= solid holdup	[—]
μ_L	= liquid viscosity	$[\text{Pa} \cdot \text{s}]$
ν	= total number of moles of ions per mole of electrolyte or 1 for non-electrolyte	[—]
ρ_L	= liquid density	$[\text{kg} \cdot \text{m}^{-3}]$
ρ_S	= solid density	$[\text{kg} \cdot \text{m}^{-3}]$
σ_L	= liquid surface tension	$[\text{N} \cdot \text{m}^{-1}]$
<Subscripts>		
est	= estimated value	
obs	= observed value	
0	= without solid particles	

Literature Cited

- 1) Akita, K. and F. Yoshida: *Ind. Eng. Chem., Process Des. Dev.*, **12**, 76 (1973).
- 2) Himmelblau, D. M.: "Process Analysis by Statistical Methods," p. 178, John Wiley & Sons (1970).
- 3) Koide, K., K. Horibe, H. Kawabata and S. Ito: *J. Chem. Eng. Japan*, **17**, 368 (1984).
- 4) Koide, K., K. Horibe, H. Kitaguchi and N. Suzuki: *J. Chem. Eng. Japan*, **17**, 547 (1984).
- 5) Koide, K., K. Kurematsu, S. Iwamoto, Y. Iwata and K. Horibe: *J. Chem. Eng. Japan*, **16**, 413 (1983).
- 6) Koide, K., H. Sato and S. Iwamoto: *J. Chem. Eng. Japan*, **16**, 407 (1983).
- 7) Koide, K., A. Takazawa, M. Kōmura and H. Matsunaga: *J. Chem. Eng. Japan*, **17**, 459 (1984).
- 8) Lamont, A. G. W.: *Can. J. Chem. Eng.*, **31**, 153 (1958).
- 9) Marrucci, G.: *Chem. Eng. Sci.*, **24**, 975 (1969).
- 10) Muroyama, K., A. Yasunishi and Y. Mitani: Proceedings of the Third Pacific Chem. Eng. Congress, **1**, 303 (1983).

(Presented in part at the 49th Annual Meeting of The Society of Chemical Engineers, Japan at Nagoya, April 3, 1984.)

LATERAL SOLID MIXING IN THE FLUIDIZED BED WITH MULTI-TUBES INTERNALS

KUNIO KATO, YUKINORI SATO, DAISUKE TANEDA
AND TAKETOSHI SUGAWA

Department of Chemical Engineering, Gunma University, Kiryu 376

Key Words: Fluidized Bed, Solid Mixing, Diffusion Model, Lateral Dispersion Coefficient, Internals, Residence Time Distribution

The lateral mixing of fluidized particles in a fluidized bed with vertical or horizontal multi-tube internals was investigated by the unsteady state behaviour of tracer particles. The behaviour of the tracer particles is analyzed by a one-dimensional diffusion model. The tracer particles were activated alumina on which zinc acetate was adsorbed. The lateral diffusion coefficient of the particles was strongly affected by the hydraulic diameter of the internals, the gas velocity and the minimum fluidized gas velocity of the particles.

Empirical equations for the lateral diffusion coefficient of the particles in a fluidized bed with vertical or horizontal multi-tube internals were obtained.

The lateral diffusion coefficient of solid particles in an ordinary fluidized bed was correlated by an empirical equation. Thermal diffusivity obtained from lateral thermal conductivity in the fluidized bed with multi-tube internals agreed with the lateral diffusion coefficient at the same fluidized conditions.

Introduction

Fluidized beds are used for drying of particles and as a solid-gas reactor such as coal combustor, regenerator of spent activated carbon or roaster of zinc blende. To analyze these processes it is very important to estimate the residence time distribution of fluidized particles in the bed.

The behaviour of fluidized particles is usually analyzed by the following models: turnover rate model,¹⁾ diffusion model^{2,3,5,6,10)} and two-phase model.¹⁾ However, the relationship between the model parameter of these models and the operating conditions of fluidized beds is not yet established.

Generally the mixing of fluidized particles in an ordinary fluidized bed is very fast, and suitable internals in the bed are quite effective in controlling the mixing rate.

Gabor⁴⁾ investigated the lateral solid mixing in a

Received October 25, 1984. Correspondence concerning this article should be addressed to K. Kato. Y. Sato is now with Isobe Works, Shinetsu Chemical Co., Ltd., Annaka 379-01. D. Taneda is now with Ōarai Nuclear Power Engineering Developing Center, JGC Co., Ltd., Ōarai, 311-13. T. Sugawa is now with Ryowa Air-Conditioning Co., Ltd.